The current issue and full text archive of this journal is available on Emerald Insight at:
https://www.emerald.com/insight/0332-1649.htm

Punching effects on local magnetic properties near the edge of nonoriented electrical steels

Changgeng Zhang and Lan Yang
Province-Ministry Joint Key Laboratory of EFEAR, Hebei University of Technology, Tianjin, China, and
Yongjian Li
State Key Laboratory of Reliability and Intelligence of Electrical Equipment, Hebei University of Technology, Tianjin, China

Received 28 January 2022
Revised 8 May 2022
Accepted 15 June 2022

Abstract

Purpose – The purpose of this study is to investigate the effect of punching on the local magnetic properties of the nonoriented electrical steel sheet.

Design/methodology/approach – A microcomposite B–H sensor consisting of a pair of B probes with a spacing of 2 mm and a 1.8 × 1.8 mm^2 H coil is designed. The region and degree of local magnetic properties degradation caused by punching can be quantitatively analyzed by flexibly moving the composite B–H sensor. The influence and physical mechanism of punching on the hysteresis loss, eddy current loss and excess loss are analyzed based on the Bertotti loss separation theory.

Findings – This study investigates the deterioration effect of the punched nonoriented electrical steel. The permeability near the edge decreases, and the core loss as well as the microhardness increases. The region of magnetic property deterioration is dependent on the area of work hardening.

Originality/value – The microcomposite B–H sensor can be used to measure the magnetic properties near the edge of electrical steel sheets under different processing conditions. This study provides the possibility of precise magnetic property model of the motor core after punching, especially valuable for motors without annealing process.

Keywords Electrical machine, Electromagnetic fields, Power losses, Magnetic device, Electromagnetic testing, Punching effects, Local magnetic properties, Nonoriented electrical steels, Loss separation

Paper type Research paper

1. Introduction

Nonoriented electrical steel is a kind of excellent soft magnetic material that is widely used in electrical motors. For high volume productions of rotor and stator laminations, the electrical steel sheets are generally punched. However, during the punching process, the residual stress produced near the punching edge deteriorates the magnetic properties of nonoriented silicon steel (Honda *et al.*, 1990). Therefore, it is important to analyze the effect of punching on the magnetic properties of electrical steel and to choose the proper magnetic property model in the design stage of motors.

Recently, the methods of investigating the influence of punching on magnetic properties were mainly based on the overall magnetic property measurement. The single-sheet tester

This work was supported in part by the National Natural Science Foundation of China, (No. 51807048, 92066206), and the Funds for Creative Research Groups of Hebei Province, (No. E2020202142).

COMPEL - The international journal for computation and mathematics in electrical and electronic engineering
Vol. 42 No. 1, 2023
pp. 159-168
© Emerald Publishing Limited
0332-1649
DOI 10.1108/COMPEL-01-2022-0064

was used to measure the magnetic properties of the processed specimens which were cut with different widths (Siebert *et al.*, 2014; Hofmann *et al.*, 2016). The effect of shearing on the core losses of nonoriented electrical steels with the thickness of 0.2–0.5 mm was measured by Epstein frame method (Naumoski *et al.*, 2014). In addition, the influences of punching on six kinds of fully processed nonoriented electrical steels with varying alloy content and grain size were studied on a 5 mm-wide annular sample (Toda *et al.*, 2014).

The precise measurement of the variation of local magnetic properties near the punching edge is crucial to the numerical modeling and the design process of motors. (Moses *et al.* 2000) analyzed the local flux density variation of the cut strips through small single-turn search coils and found that the degraded depth from the punching edge could be up to 15 mm depending on the material type. Harstick *et al.* (2014) applied a probe with a high spatial resolution to detect the influence of cutting tool wear on local magnetic properties. The probe is used for micromagnetic, multiparameter microstructure and stress analysis. Wang *et al.* designed a *B–H* vector sensor composed of a pair of *B*-probes and a high-precision Hall element to realize the reproducible nondestructive and flexible measurement of the local magnetic properties (Wang *et al.*, 2018).

In this study, a microcomposite *B–H* sensor is designed to accurately investigate the variation of local magnetic properties near the punching edge. The composite sensor consists of a pair of *B* probes with a spacing of 2 mm and a 1.8×1.8 mm^2 *H* coil. The combination of the composite sensor along with a three-dimensional mobile device allows the flexible motion of measurement location to measure the magnetic properties at any position of the sample. The region and degree of magnetic property deterioration are quantitatively investigated, and the microscopic mechanism of loss variation is analyzed based on the Bertotti loss separation theory.

2. Sample preparation

The size of the motor stator which accounts for the largest industrial share generally ranges from 20 to 60 mm. The cold-rolled nonoriented electrical steel B35A270 is punched into a square shape with the size of 49.5×49.5 mm^2. Two samples with different punching stress are analyzed. Sample 1 is punched by 80 MPa punching pressure and Sample 2 is punched by 250 MPa punching pressure. The punching speed is 12 times/min and the punching clearance is 25 μm.

3. Microhardness distribution

The microhardness distribution of the center line perpendicular to the punching edge is measured using an HMV-2T microhardness tester which loading lasts 15 s with a maximum force of 0.98 N. The measurements are conducted with a Vickers indenter. Indentation is performed in a row starting from the edge of the sample toward the center with a spacing of 0.25–1 mm between the indents. It is necessary to polish the sample before the measurement because the insulating coating on the surface will affect the measurement results.

The microhardness distribution near the edge with different punching stresses is shown in Figure 1. The microhardness near the edge is observed to be higher indicating the existence of plastic deformation. The maximum edge microhardness increases up to 249 HV at 80 MPa and 301 HV at 250 MPa, corresponding to the hardening depth up to about 4 and 10 mm from the edge. The uneven deformation and punching stress cause residual stress and the deterioration of toughness. When the samples are plastically deformed, the mechanical energy applied to the silicon steel material is absorbed by the lattice through the appearance of microstructural defects (Melkebeek, 2003). The increased dislocation density further functions as the pinning site for the domain wall motion, which degrades the magnetic properties.

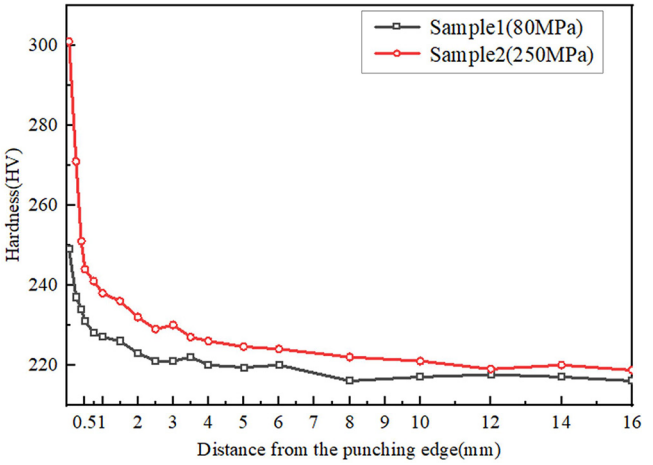


Figure 1.
Hardness near the edge under different punching stress

Compared to the region away from the punching edge, the microhardness of both samples increases sharply within the region of 2 mm from the edge and then decreases slowly within a large zone until it remains stable at 4 and 10 mm, respectively. In the large affected zone, the small increase in hardness may be affected by the movement of the sheet along the punching die during the separation process.

4. Magnetic experiment

The excitation structure of the local magnetic property test system integrated with a three-dimensional mobile device is shown in Figure 2 (Yang *et al.*, 2014). The sample is placed between the magnetic poles of the C-shaped core. The microcomposite *B–H* sensor is specially designed for measuring local magnetic properties at different positions near the punching edge. The needle probes are used to measure the *B* signal in the magnetization direction. To meet the requirement of edge local measurement, the probe distance should be as small as possible. However, the measurement accuracy of needle probe method decreases with the decrease of probe distance. To select the optimal probe distance, the variation of measurement accuracy with probe distance is studied. The structure and distance of *B* needle probe are shown in Figure 3. The distance between the needles ranges from 2 to 20 mm with 2 mm step, and the magnetic flux density ranges from 0.6 to 1.6 T with 0.1 T step. Because the error decreases with the increase of needle distance *d*, the magnetic flux

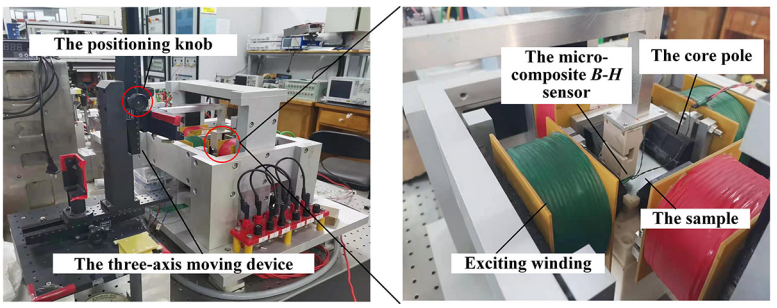


Figure 2.
Excitation structure of the magnetic property test system

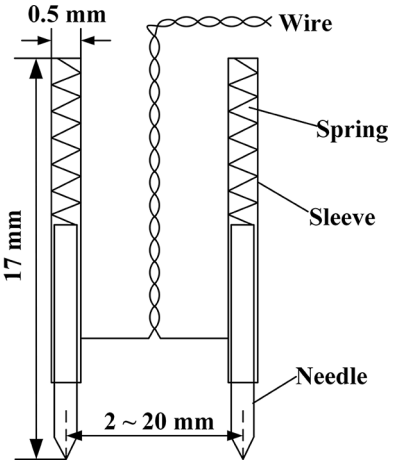


Figure 3.
Schematic structure of *B* probe

density measured by the 20 mm distance needle is taken as the reference value which is compared with ones measured by the other distances needles.

Figure 4 shows the relative error of magnetic flux density is negatively correlated with the probe distance. The relative error is 1.75%–2.94% when the distance is reduced to be 2 mm, which can also be practical and effective in the engineering core loss measurements. Therefore, the *B* probe is set as 2 mm to ensure the measurement accuracy and to satisfy the local magnetic flux density test requirements.

Considering the *B* probe distance, the size of the *H* coil is designed as 1.5×1.5 mm^2, which is used to measure the local *H* signal in the direction of magnetization. The schematic structure and physical image of the composite sensor are shown in Figure 5. The *H* coil is wound on the first piece of 0.5 mm-depth PCB, and the upper and lower layers are overlappedly wound to effectively reduce electromagnetic interference. The two retractable *B* probes with 2 mm distance are fixed on the other piece of PCB. The two pieces of PCB are

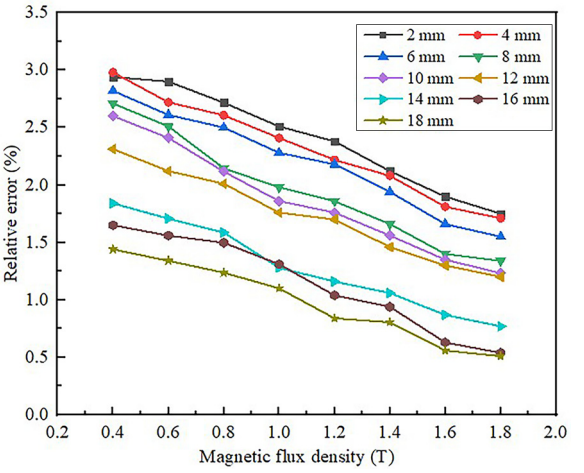


Figure 4.
Variation of relative error with probe distance

bonded together to form a composite sensor. The composite B–H sensor should be close enough to the sample surface to acquire the correct induction voltage values. Based on Faraday's law, the B and H signals can be calculated from the measured induction voltages of the B probes and H coil. They can be expressed as:

$$B = \frac{2}{bd}\int V_B dt \tag{1}$$

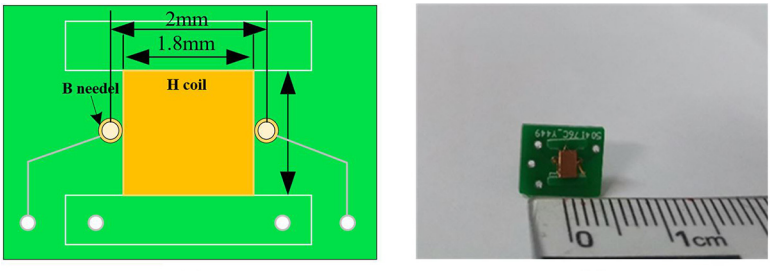
$$H = \frac{1}{\mu_0 K_H}\int V_H dt \tag{2}$$

where b is the distance between probes, d is the thickness of the sample, K_H is the coil coefficient of H coil obtained by calibration in a long solenoid and V_B and V_H are the induced voltages of the B probes and H coil, respectively.

To verify the measurement accuracy of the composite B–H sensor, the core loss measured by the composite sensor is compared with the loss measured by the Epstein frame at 50 Hz according to IEC60404-2, as shown in Figure 6. It can be seen that the loss curves of the two methods are almost the same. The maximum error is less than 5% ranging from 1.0 to 1.5 T, while the average error is only 3.3%, which verifies the measurement accuracy of the composite B–H sensor.

The uniformity of the magnetic induction in the measurement region is important to the test. Thus, based on the finite element method, the magnetic induction distribution B of the sample is simulated as shown in Figure 7. The distance between the sample and the magnetic pole is set as 0.25 mm according to the test. The result indicates that the B is unevenly distributed in the strip region of the sample near the pole, but evenly distributed in other regions. To study the difference in local magnetic properties between the punching edge and the central region, it is necessary to ensure the magnetization of the two regions is the same. Therefore, the center line perpendicular to the magnetization direction of the sample is taken as the measurement line. The rolling direction of the sample is parallel to the magnetization direction, and an AC magnetic field with a frequency of 20–200 Hz is applied along the rolling direction.

The flexible movement of the composite sensor is realized by a three-dimensional mobile device which has a connecting rod that can move the sensor into the air gap of the magnetic pole. The position of the composite sensor in x, y and z directions can be adjusted by the positioning knob of the three-dimensional mobile device. The normal pressure applied to the composite sensor is adjusted to ensure that the H coil and B probes are closely touched with



(a) (b)

Figure 5.
(a) Schematic structure and (b) physical image of the composite B-H sensor

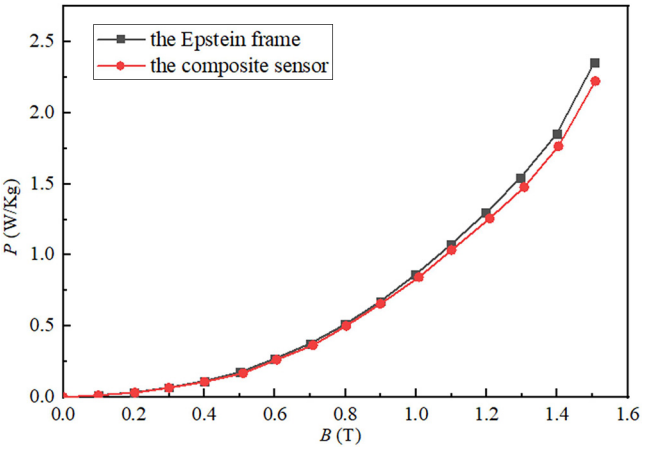


Figure 6.
Verification of the composite sensor

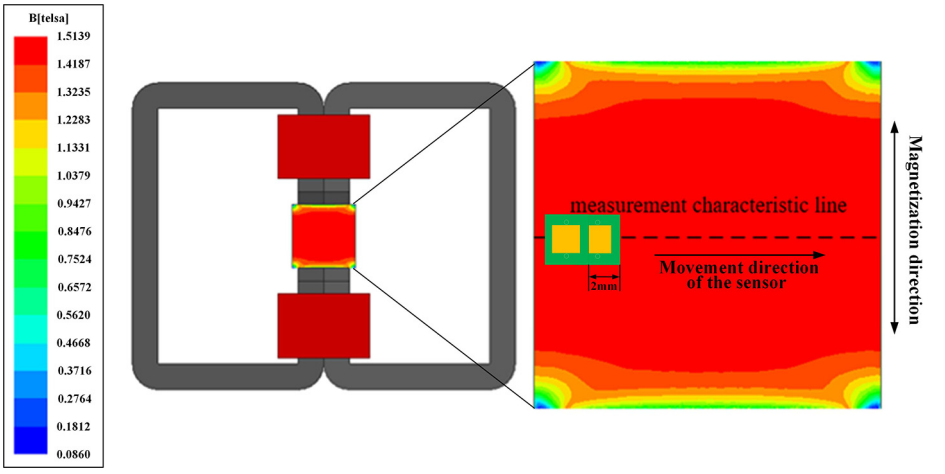


Figure 7.
Magnetic circuit and distribution of magnetic induction B on the sample surface

the sample. According to the condition of magnetic field interface, the tangential component of magnetic field intensity on both sides of the interface of the two magnetic mediums is continuous. When the H coil is infinitely close to the sample surface, the magnetic field measured by H coil is the magnetic field in the sample. The movement of the composite sensor can be realized to obtain the local magnetic properties at different positions near the punching edge.

5. Analysis of hysteresis loops

When Sample 1 and Sample 2 are magnetized to 1.6 T at 50 Hz, the hysteresis loops at different positions are shown in Figure 8. It indicates that the hysteresis curve is much slender in the horizontal direction in the vicinity of the punching edge. Compared with the central region, the magnetization of the sample up to 1.6 T requires larger H at the punching edge (1,500 A/m for Sample 1 and 1,880 A/m for Sample 2). The hysteresis curves measured

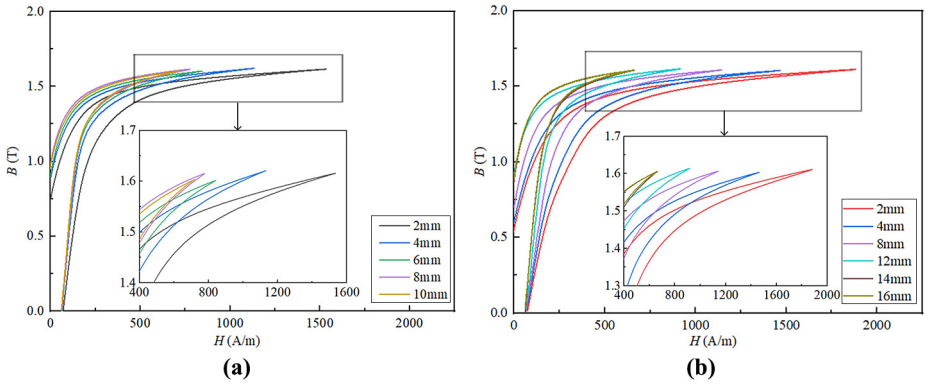


Figure 8.
Hysteresis loops at 1.6 T, 50 Hz of the samples

Notes: (a) Sample 1; (b) Sample 2

away from the sample edge almost coincide with each other. As a result, the magnetic properties in this region are not affected by punching.

Under the same magnetic field H, the magnetic induction B decreases with the decrease of the distance from the edge. The region where B decreases is regarded as the degradation region. The deterioration region of Sample 1 is within 6 mm from the edge, and that of Sample 2 is within 12 mm from the edge. In addition, the magnetic properties of the two samples deteriorate significantly within 2 mm from the edge, corresponding to the region where the microhardness increases sharply. Outside of the region, the gradient of microhardness with the distance to the punched edge is much smaller than that inside the region, while the magnetic property is very close to that in the center of the punched silicon steel, indicating the influence of punching on nonoriented silicon steel can be neglected. It illustrates that the residual stress of the punching edge leads to the deterioration of magnetic properties, and the region of magnetic property deterioration is dependent on the area of work hardening.

Compared with the 80 MPa punching stress, the impact of 250 MPa punching stress on hysteresis loops is more significant. When the punching edge of the sample is magnetized to 1.6 T, the applied H required by Sample 2 is about 1.25 times that by Sample 1, and the magnetic deterioration region of Sample 2 is about twice that of Sample 1.

6. Analysis of power loss

The power losses at different positions of the two samples at 50 Hz are illustrated in Figure 9. The results indicate that the core loss increases rapidly with the increase of magnetic field H and the loss near the punching edge is higher than that at the center. The loss of Sample 1 increases by 0.9%–15.25% within 6 mm from the edge at 1.5 T. The loss of Sample 2 increases by 6.8%–29.55% at 1.5 T. Compared with Sample 1, the region of increased loss is extended by 6 mm inward.

The Bertotti theory is a loss separation model, which can be used to investigate the mechanism for loss variation after punching. The core loss of the punched sample can generally be separated into three components: hysteresis loss, classical eddy current loss and excess loss. Then, the energy loss per cycle P/f can be expressed as:

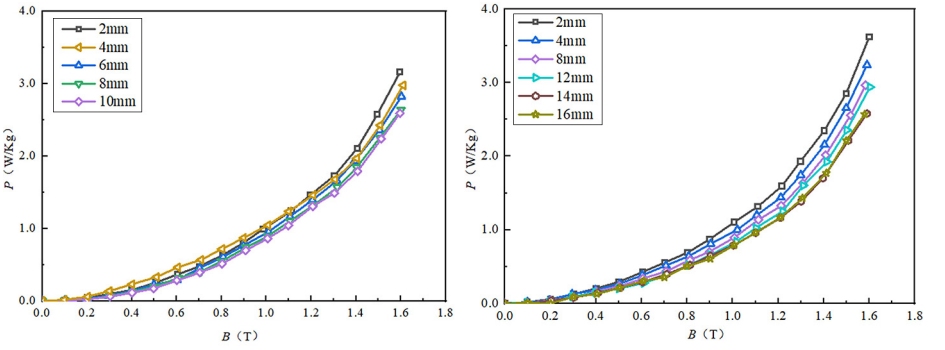


Figure 9.
Core losses of the two samples

Notes: (a) Sample 1; (b) Sample 2

$$\frac{P}{f}(B,f) = k_h(B)\frac{1}{\rho} + k_c(B)f + k_e(B)f^{0.5} \tag{3}$$

where k_h, k_c and k_e are the hysteresis coefficient, classical eddy current coefficient and excess loss coefficient, respectively (Li, 2016). The value of k_h, k_c and k_e under specific B and f can be determined by nonlinear fitting.

The P/f–f curve at 1.4 T of Sample 1 with punching pressure of 80 MPa is shown in Figure 10. It indicates that the longitudinal intercept of the P/f–f curve increases with the decrease of the distance from the edge, that is, the hysteretic loss increases. The slope of the straight part of the curve is almost constant, indicating the eddy current loss is almost unchanged. The k_h, k_c and k_e are determined by fitting the experimental loss of 20–200 Hz, which play an important role on the loss prediction of the three components at specific magnetic induction.

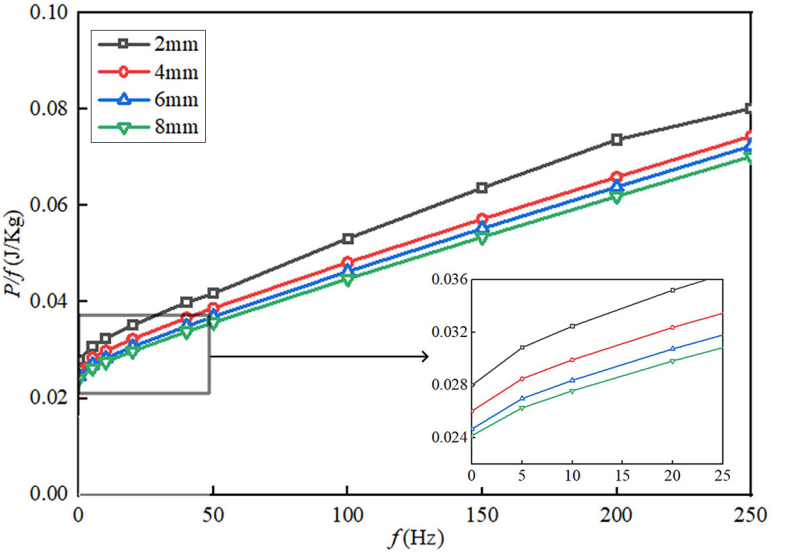


Figure 10.
P/f–f curve at 1.4 T of Sample 1

Figure 11(a) and (b) shows the influence of punching on the three loss components of Sample 1 at 0.8 and 1.4 T with the frequency of 50 Hz. Obviously, the hysteresis loss accounts for the main part of the total loss. Both hysteresis loss and excess loss increase after punching, and the excess loss (45.56% increase at 0.8 T, 54% increase at 1.4 T) increases more than the hysteresis loss (12.95% increase at 0.8 T, 15.07% increase at 1.4 T).

From the microscopic point of view, the hysteresis loss is caused by the movement of magnetic domain wall in the magnetization process. Because of the increase of residual stress and pinning sites near the punching edge, the number of movable magnetic domains decreases (Senda, 2011), and the motion resistance of magnetic domains increases, leading to the increase of hysteresis loss.

The eddy current loss is less affected by punching, which is mainly related to the conductivity and thickness of silicon steels insensitive to the residual stress. The excess loss is based on the movement of the magnetic domain walls. Punching makes the magnetic domains of the nonoriented electrical steel wider (Cao, 2016). The velocity of domain wall motion is proportional to the moving distance at the same frequency. Therefore, the excess loss increases with the increase of the magnetic domain width.

7. Conclusions

The effect of punching process on microhardness and local magnetic properties has been systematically investigated. The results show that the microhardness of both samples increases sharply in the range of 2 mm indicating the occurrence of plastic deformation and residual stress, and the hardened region from the punching edge is 4 mm at 80 MPa and 10 mm at 250 MPa. A microcomposite *B–H* sensor with the *B* probe distance of 2 mm is designed to obtain the region and degree of magnetic property deterioration of the punched silicon steel sheet. An increase in core loss due to punching is observed to be 0.9%–15.25% for 80 MPa and 6.8%–29.55% for 250 MPa at 1.5 T, corresponding to a deterioration area extending up to a distance of 6 and 12 mm from the punching edge, respectively. The region of magnetic deterioration is dependent on the region of increased microhardness. The punching process of nonoriented electrical steel produces an increase of both hysteresis loss and excess loss, and the excess loss increases larger than the hysteresis loss. This paper provides the possibility of precise magnetic properties model of the punched motor core, especially valuable for motors without annealing process.

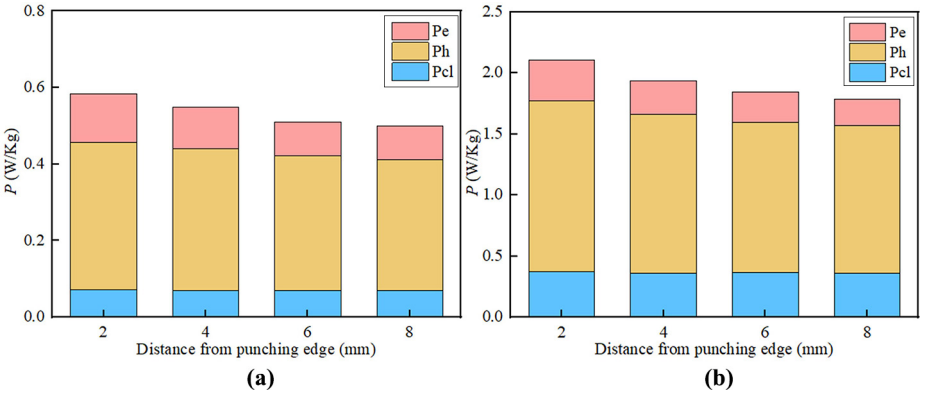


Figure 11. Hysteresis loss, eddy current loss and excess loss at different distances from the edge of Sample 1: (a) 0.8 T and (b) 1.4 T

References

Cao, H., Hao, L. and Yi, J. (2016), "The influence of punching process on residual stress and magnetic domain structure of non-oriented silicon steel", *Journal of Magnetism and Magnetic Materials*, Vol. 406 No. 5, pp. 42-47.

Harstick, H.M., Ritter, M. and Riehemann, W. (2014), "Influence of punching and tool wear on the magnetic properties of nonoriented electrical steel", *IEEE Transactions on Magnetics*, Vol. 50 No. 4, pp. 1-4.

Hofmann, M., Naumoski, H. and Herr, U. (2016), "Magnetic properties of electrical steel sheets in respect of cutting: micromagnetic analysis and macromagnetic modeling", *IEEE Transactions on Magnetics*, Vol. 52 No. 2, pp. 1-14.

Honda, A., Fukuda, B. and Ohyama, I. (1990), "Effects of magnetic properties of non-oriented electrical steel sheets on motor efficiency", *Journal of Materials Engineering*, Vol. 12 No. 1, pp. 41-45.

Li, Y.J., Cao, L. and Zhang, C.G. (2016), "Rotational core loss of silicon steel laminations based on three-dimensional magnetic properties measurement", *IEEE Transactions on Applied Superconductivity*, Vol. 26 No. 4, pp. 1-5.

Melkebeek, B.J. (2003), "Induced stresses due to the mechanical cutting of non-oriented electrical steels", *Journal of Magnetism and Magnetic Materials*, pp. 355-357.

Naumoski, H., Maucher, A. and Vandenbossche, L. (2014), "Magneto-optical and field-metric evaluation of the punching effect on magnetic properties of electrical steels with varying alloying content and grain size", *2014 4th International Electric Drives Production Conference (EDPC)*, pp. 1-9.

Senda, K., Fujita, A. and Honda, A. (2011), "Magnetic properties and domain structure of non-oriented electrical steel under stress", *IEEJ Transactions on Fundamentals and Materials*, Vol. 131 No. 10, pp. 884-890.

Siebert, R., Schneider, J. and Beyer, E. (2014), "Laser cutting and mechanical cutting of electrical steels and its effect on the magnetic properties", *IEEE Transactions on Magnetics*, Vol. 50 No. 4, pp. 1-4.

Toda, H., Zaizen, Y. and Namikawa, M. (2014), "Iron loss deterioration by shearing process in non-oriented electrical steel with different thicknesses and its influence on estimation of motor iron loss", *IEEJ Journal of Industry Applications*, Vol. 3 No. 1, pp. 55-61.

Yang, Q.X., Li, Y.J. and Zhao, Z. (2014), "Design of a 3-D rotational magnetic properties measurement structure for soft magnetic materials", *IEEE Transactions on Applied Superconductivity*, Vol. 24 No. 3, pp. 1-4.

Further reading

Rygal, R., Moses, A.J. and Derebasi, N. (2000), "Influence of cutting stress on magnetic field and flux density distribution in non-oriented electrical steels", *Journal of Magnetism and Magnetic Materials*, Vols 215/216 No. 216, pp. 687-689.

Wang, Z., Zhang, Y.L. and Ren, Y.J. (2018), "Design and implementation of detection system of local magnetic property on the surface of iron core", *Transactions of China Electrotechnical Society*, Vol. 33 No. 23.

Corresponding author

Changgeng Zhang can be contacted at: changgeng.zhang@hebut.edu.cn

For instructions on how to order reprints of this article, please visit our website:
www.emeraldgrouppublishing.com/licensing/reprints.htm
Or contact us for further details: **permissions@emeraldinsight.com**